LOW-AMPLITUDE ACOUSTIC MODULATION AS A TOOL FOR CONTROLLING THE VORTEX STRUCTURES OF THE TURBULENT AXISYMMETRIC AIR JET

Nikola ĆETENOVIĆ[2], Dejan CVETINOVIĆ[1], Aleksandar ERIĆ[2], Đorđe ČANTRAK[3], Jaroslav TIHON[4], Kazuyoshi NAKABE[5], Kazuya TATSUMI[5]

[1] Corresponding Author. University of Belgrade, VINCA Institute of Nuclear Sciences, Laboratory for Thermal Engineering and Energy, Belgrade, Serbia, Tel.: +381 63 8433 988, E-mail: deki@vin.bg.ac.rs

[2] University of Belgrade, VINCA Institute of Nuclear Sciences, Laboratory for Thermal Engineering and Energy, Belgrade, Serbia e-mail: nikola.cetenovic@vin.bg.ac.rs

[3] Faculty of Mechanical Engineering, University of Belgrade, Belgrade, Serbia, djcantrak@mas.bg.ac.rs

[4] Institute of Chemical Process Fundamentals, Academy of Sciences of the Czech Republic, Prague, Czech Republic e-mail: tihon@icpf.cas.cz

[5] Mechanical Engineering, Faculty of Engineering, Kyoto University, Kyoto, Japan, e-mail: tatsumi@me.kyoto-u.ac.jp

ABSTRACT

The roll-up of vortex structures in turbulent jets can be influenced by low-amplitude modulations of the nozzle exit velocity. These modulations can be generated either by external low-amplitude oscillations or by self-sustaining oscillations inherent to the operation of specially designed whistler nozzles. The aim of the experimental investigations, mathematical modeling, and numerical simulations carried out as part of the project evaluation was to thoroughly investigate the characteristics and vortex dynamics of acoustically modulated and non-modulated nozzles. A major focus was on identifying effective methods to control vortex structures, as these play an important role in improving heat transfer processes.

This paper presents the results of mathematical modeling and numerical simulations of free and impinging turbulent axisymmetric air jets, both unmodulated and modified by low-amplitude oscillations. The modeling results showed strong agreement with experimental findings confirming the ability to manipulate vortex structures in the jet by acoustically modulating the nozzle exit velocity. This study provides a basis for the development and optimization of technological processes using air jets, particularly in applications where improved heat transfer is critical.

Keywords: Impinging jet, flow control, heat transfer, mathematical modelling, turbulent axisymmetric air jet, vortex structures.

NOMENCLATURE

D	$[m]$	diameter of the nozzle
L	$[m]$	distance of the impact plate from the nozzle exit along the jet axis
Nu	$[-]$	Nusselt number
Pr	$[-]$	Prandtl number
Re	$[-]$	Reynolds number
Re_t	$[-]$	Reynolds number of vortex structures
St_D	$[-]$	Strouhal number of the jet
T	$[K \ or \ °C]$	temperature
U	$[ms^{-1}]$	mean velocity
f	$[Hz]$	frequency
h	$[Wm^{-2}K^{-1}]$	heat transfer coefficient
p_w	$[Pa]$	wall pressure
q_c	$[Wm^{-2}]$	heat flux from the heated surface
r	$[m]$	radial distance from the jet axis
t	$[s]$	time
u'	$[ms^{-1}]$	velocity fluctuation
x	$[m]$	distance in the x-axis direction
x_2	$[m]$	distance from the impact surface toward the nozzle
y	$[m]$	distance in the y-axis direction
λ	$[Wm^{-1}K^{-1}]$	thermal conductivity of the fluid
v	$[m^2s^{-1}]$	kinematic viscosity
τ_w	$[Pa]$	wall shear stress
σ_{ij}	$[Pa]$	total stress

1. INTRODUCTION

Impinging jets is a widely used as a way to provide an effective and flexible transfer of energy or mass in diverse industrial applications. Liquid or gaseous flow released against a surface can efficiently transfer thermal energy or mass between the surface and the fluid. Heat transfer applications include cooling during material forming processes, heat treatment of different materials, cooling of electronic components, heating of surfaces for defogging, cooling of turbine components, cooling of critical machinery structures, and many other similar industrial processes. Typical mass transfer applications include drying and removal of small surface particulates. Abrasion and heat transfer are interesting for vertical/short take-off and landing jet devices in the case of direct lift propulsion systems. The heat transfer rate can be assumed as a complex function of many parameters: Reynolds number (Re), Prandtl number (Pr), the non-dimensional nozzle to plate spacing (L/D), and the non-dimensional displacement from the stagnation point (r/D), also nozzle geometry, flow confinement, initial turbulence intensity of the jet, dissipation of jet temperature, etc. [1], [2], [3], [4], [5]. Vortex structures of impinging jet are confirmed by a number of authors to have great importance in the impinging jet heat transfer. Primary vortices, which roll-up in the jet shear layer, induce an unsteady flow separation at the wall, prohibiting the heat transfer between the wall and the fluid jet. Thus, controlling of them necessary leads to the control of the heat transfer from the jet to the wall, and vice versa. It is found that the vortex roll-up can be controlled by adding small amplitude modulation of the nozzle exit velocity.

Subject of present work is submerged, round, unconfined impinging air jet, issuing from a bell-shaped converging nozzle [6], [7] and from the specially designed whistler nozzle [8]. The aim of the investigation is to qualitatively describe the vortex structure of the free and impinging jet and to examine the possibility of its control by low-amplitude modulation of the nozzle exit velocity by external source of sound and self-sustained resonant sound oscillations generated in the operation of the whistler nozzles. The vortex roll-up is generally triggered by a perturbation of the shear layer, which is amplified by the shear layer instability [9], [10]. The perturbation can also be a random noise wave arriving from the environment, from an upstream flow system, or from a downstream flow event. The modulation of the nozzle exit velocity acts as an additional source of disturbances, which overwhelms the natural disturbances if the modulation is strong enough. Modulation of the nozzle exit velocity controls the vortex roll-up and hence all structure of the turbulent axisymmetric jet [11], [12].

2. EXPERIMENTAL RESULTS

Series of measurements along the jet centreline and in the plane normal to the jet at the nozzle exit is provided, to explore influence of the small amplitude perturbation to the structure of free turbulent axisymmetric air jet issuing from a bell-shaped nozzle [6], [7].

The experimental configuration used for measuring the flow field in the impinging jet system is schematically depicted in Figure 1. It comprised a bell-shaped converging nozzle, a settling chamber, a flow disturbance mechanism, an impingement plate positioned perpendicular to the jet axis, an air supply system, and a control and data acquisition system. The bell-shaped nozzle, constructed from a plastic material, had an outlet diameter of 25 *mm*. Air entered the settling chamber via two centrally located pipes, subsequently passing through four grids and a honeycomb structure. The final section of the settling chamber was equipped with both a pressure tap and a temperature sensor.
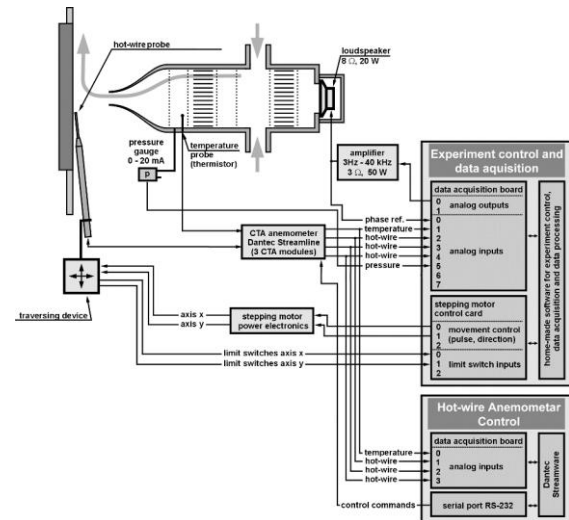

Figure 1. Experimental setup for experiments in an impinging jet configuration

Air jet normalized velocity profiles and normalized velocity r.m.s. profiles at the free jet centreline are shown on the Figure 2. The profiles were measured up to $L=8D$ downstream distances from the nozzle lip. Figure 2. shows the change in the normalized velocity and velocity r.m.s. profiles along the jet axis for a fixed Reynolds number, $Re=10000$, different excitation Strouhal number, $St_D=0.3$-2.12, and excitation amplitude in the range $u'/U_e=1$-3%.

From presented figures can be clearly distinguished four ranges of Strouhal number where jet behaviour can be considered as very similar. First excitation Strouhal number range is around naturally most amplified mod of excitation (called "preferred mode", [3]), $St_D \approx 0.3$. Second belongs to the
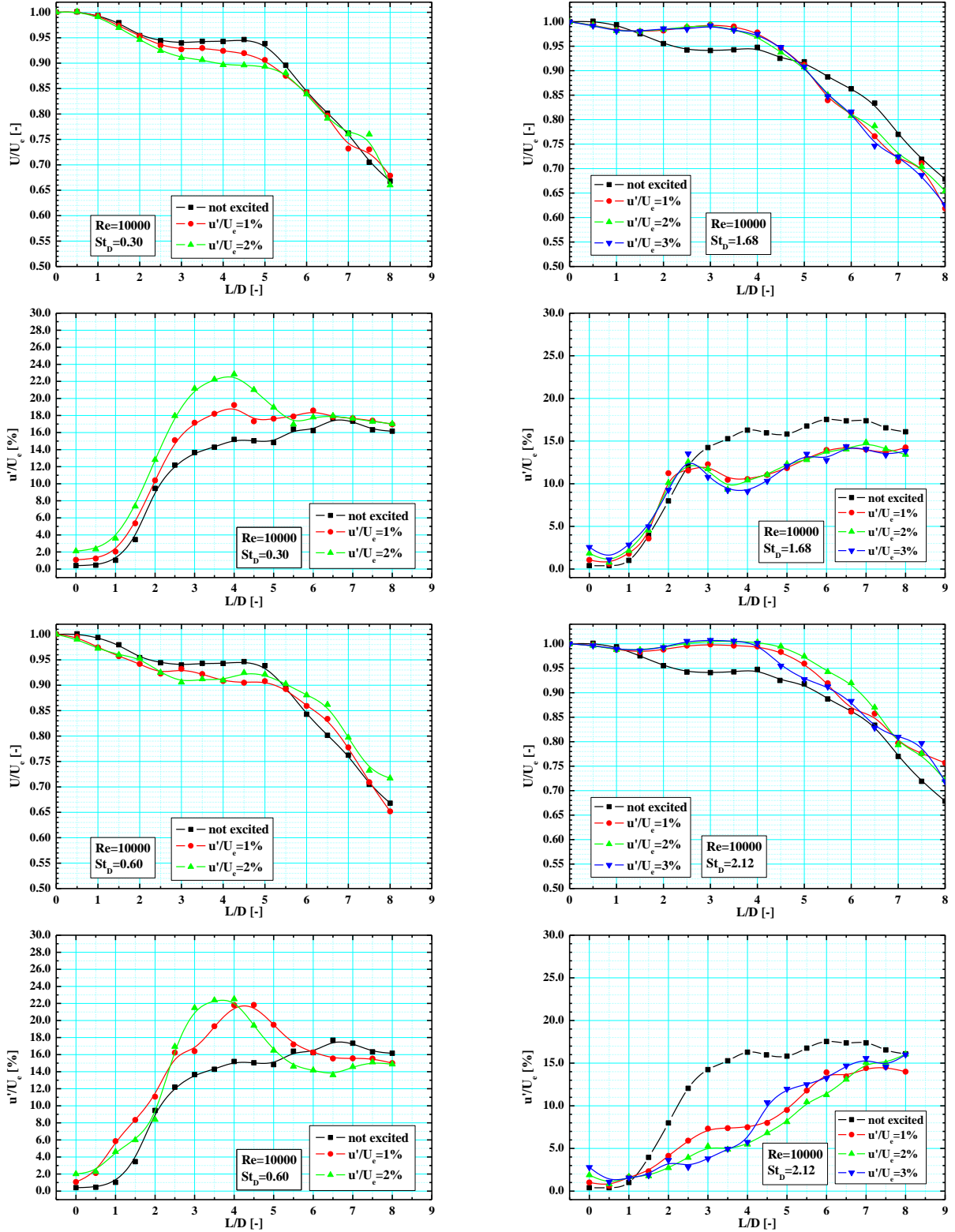
Figure 2. Normalized velocity and velocity r.m.s. profiles along the jet centreline; – flow and excitation conditions: *Re*=10000; *St_D*=0.3-2.12; *u′/U_e*=1-3%

frequency range around double most amplified mod value, St_D≈0.6-0.7, denoted in the literature as a stable vortex pairing mode. Third excitation Strouhal number range are values around St_D≈1.0 and fourth is above St_D≈1.8. All excitation modes have their own characteristics that can be explored more deeply.

Looking at the normalized velocity profiles in the excitation Strouhal number range around naturally most amplified mode, St_D=0.2-0.4, can be obviously seen that excitation make influence in shortening of the jet potential core, from previous value between 4.5 and 5 nozzle diameters to value between 3 and 4 diameters, depending on the excitation amplitude. From the shape of the normalized velocity one can conclude that potential core still exists, but peripheral vortices, grown in size, can be found in the centreline on smaller axial distance from the nozzle lip.

Second excitation Strouhal number range, St_D=0.5-0.8, denotes stable vortex pairing mode of excitation, is characterized by more sudden decrease in the jet potential core length. Peak in the normalized velocity r.m.s. appear at the smaller axial distance from the nozzle lip at a slightly higher value than in the previously described excitation range, which coincides with the conclusion that the jet potential core disappears on smaller axial distance. Increase in the excitation amplitude does not produce significant increase in the normalized velocity r.m.s. profile, like some kind of saturation exists. This fact can be explained by redistribution of the energy in the jet faced with a vortex pairing, and high amount of energy used for this process.

Range of excitation around Strouhal number St_D≈1.0, is characterized with a high intermittency and unstable behaviour. Jet potential core is somehow extended, and normalized mean velocity at the jet centreline increased, but depending on the excitation condition some big difference between very close measuring points is found and repeated so many times in experiments. This discontinuity clearly seen in the normalized velocity r.m.s. profiles look like some discrete "jumps" from one jet behaviour to another, from one frequency regime to another.

Excitation in the range above St_D≥1.8, has produced higher velocities in the areas at the higher axial distance from the nozzle lip and significant decrease in the normalized velocity r.m.s. comparing to the not excited case, especially in the excitations with a Strouhal numbers above St_D≥2.0. Influence of excitation amplitude here is negligible in both normalized velocity profiles and normalized velocity r.m.s. profiles in all investigated excitation amplitude range.
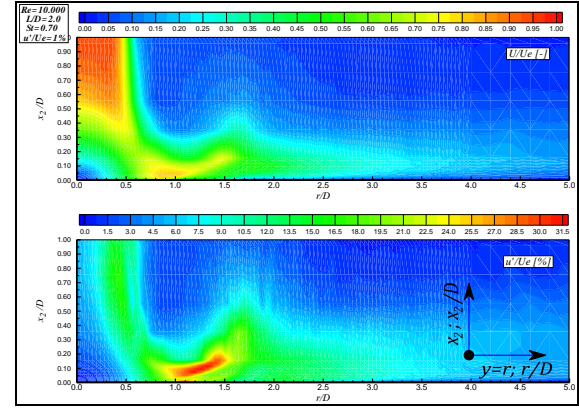

Figure 3. Normalized mean velocity and turbulence intensity fields in the area 1Dx5D above impinging surface - with the sound excitation; Re=10000; St_D=0.7; u^j/U_e =1%; L/D=2

Figure 3. shows the fields of normalized velocity, and turbulence intensity of the modified axisymmetric turbulent jet of Reynolds number Re = 10000 with excitation Strouhal number St_D=0.7 and the initial amplitude of the oscillations u^j/Ue = 1%. The jet impinges to the flat surface placed perpendicular to the jet axis at an axial distance L/D=2. Measurement results are extracted from very intense net measurements with a hot wire anemometry in the area 1Dx5D above the impinging surface. In spite of jet velocity reduction, as a consequence of sound modification, the profile of the normalized velocity shows great resemblance to the profile of the unmodified stream and the same flow characteristics for the same impinging distance. Jet slightly accelerated on the path around stagnation zone and vortices from the jet shear layer descend into the boundary layer at the wall of the impinging surface, causing the separation streamline at the same radial distance that we observed in the experiments without sound modification. In the turbulence intensity field can be observed intensification of the vortical structures in the shear layer close to the impinging surface, which is accompanied by abrupt changing of the flow direction and acceleration of the flow around the stagnation zone.

Figure 4. illustrates the process of vortex penetration from the jet shear layer into the boundary layer flow on the wall of the impinging surface. Induced velocity angle between the wall and ejected vortex path depends on the speed of rotation of the incoming vortex.
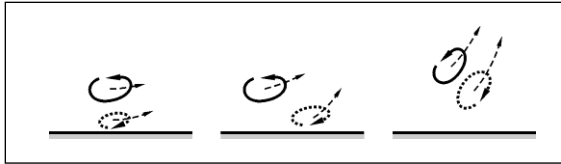
Figure 4. Vortex approaching boundary layer on the impinging surface (injective phase). The primary vortex - a solid line; spot - the secondary vortex; dash-line - induced velocity from the wall (ejective phase)

The analysis of the presented turbulence intensity field, Figure 3., which corresponds to the case of Strouhal number $St_D = 0.7$ modification, it can be argued that the angle at which the vortex ejects from the impinging surface is greater with respect to the rest of the modification cases investigated. In this mode, the excitation leads to the stable pairing of vortices and the newly formed vortex created in the process of pairing is stronger, with the higher rotation speed, which leads to a larger bounce angle.

The measurement of velocity field in the case of Strouhal number modification $St_D = 2.01$ is shown in Figure 5. The results confirm the specificity of this modification. Specifically, this case of modification is not characterized with injective and ejective movement of vortices near the impinging surface shown on previous figure. A series of vortices formed in the shear layer of the jet near the impinging surface are with lower vorticity and vortices are not powerful enough to initiate this phenomenon. Stream lines do not separate from the impinging plate wall, even flow was accelerated around stagnation zone, causing uniformity in a turbulence intensity profile on a large range of radial distances from the axis of the jet. The influence of the initial amplitude of the sound oscillations in the jet in this particular excitation Strouhal number range is negligible, so that the modification of the $u'/Ue =3\%$, shown in Figure 5., are not significantly different from the cases of lower-amplitude external excitation investigated.

From the standpoint of controlling fluid structure with the help of external acoustic modifications this Strouhal number range looks most suitable. Very uniform zone of turbulence intensity, which has been verified for all investigated axial distances between the nozzle lip and impinging surface, can be considered as very predictable characteristic controlled by sound modifications with Strouhal number $St_D \geq 2.0$. Here, however, must be noted that the realization of such high value Strouhal number in the special nozzle design that produce self-sustained oscillation – whistler nozzle, can be very difficult.
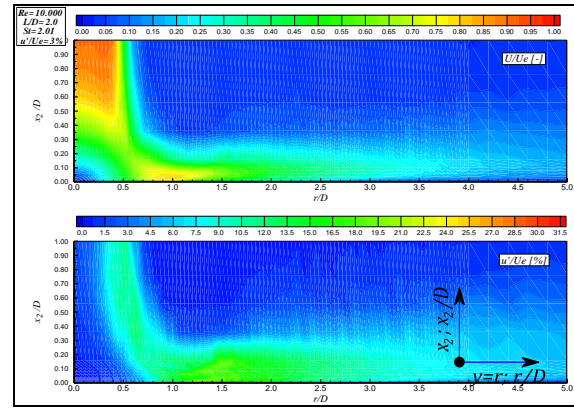

Figure 5. Normalized mean velocity and turbulence intensity fields in the area 1Dx5D above impinging surface - with the sound; Re=10000; St_D=2.0; u'/U_e =3%; L/D=2

As part of the experimental investigations, visualization of the free jet emerging from the nozzle was also performed. The studied cases correspond to Strouhal numbers of 0, 0.3 and 0.52, while the Reynolds number was 91000 and the nozzle diameter was 18 mm. The presented images (Figure 6.) were obtained using a PIV (Particle Image Velocimetry) system. The recorded jet length was 7D.

In the first image, corresponding to the unexcited jet, it can be observed that the potential core, characterized by an unchanged velocity relative to the nozzle exit, contracts and vanishes at axial distances of $L/D \geq 5$.
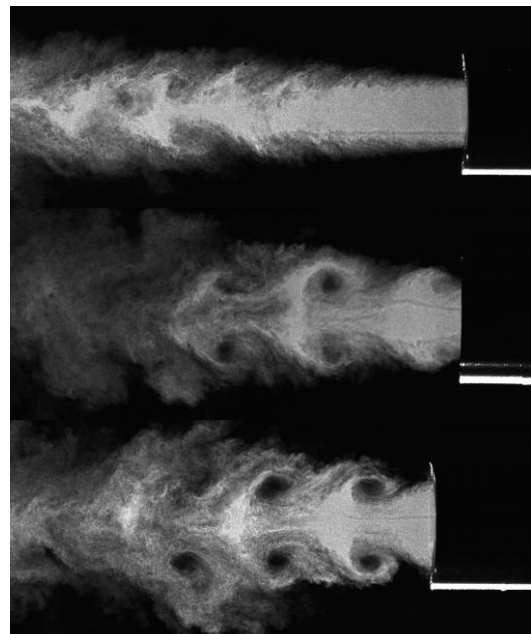

Figure 6. Visualization of the free jet at Reynolds number Re = 91000 for Strouhal numbers St_D = 0 (top image), St_D = 0.3 (middle image) and St_D = 0.52 (bottom image)

In the second image, it is evident that excitation with a Strouhal number of $St_D = 0.3$ (close to the "preferred" excitation mode) generates vortex structures in the form of highly regular vortex rings with high rotational velocity around the vortex core. The potential core is significantly shorter, and pronounced axial oscillations can be observed.

The third image shows the case with excitation at $St_D = 0.52$, where the potential core is longer than in the previous case. The large vortices are not regular in shape, because they are formed by the pairing of multiple vortex structures along their path from the nozzle exit. At smaller axial distances from the nozzle exit, this case of excitation leads to more pronounced radial spreading of the jet, which has also been confirmed by hot-wire anemometry velocity measurements.

3. MATHEMATICAL MODELLING

In most of practical engineering situations the impinging jets are modelled using different turbulent models. As already pointed out by many researchers, the most of the turbulence models were developed for flows, which are parallel to the wall. Therefore, their applicability to impinging jet is limited because of significant differences from parallel flows:

– kinetic energy of turbulence in the vicinity of the axis of symmetry (i.e. stagnation point) is generated by the normal stresses (for flows parallel to the wall this role have shear stresses);
– the velocity fluctuation component normal to the wall is of the same order, or even larger than the component parallel to the wall; in parallel flows, the normal component is much smaller;
– the local turbulent length scales near the wall are strongly affected by the length scale of jet turbulence; in parallel flows, the length scales are determined by the distance from the wall;
– in impinging jets, there is an important convective transport of turbulence toward the stagnation point; in parallel flow, the convective transport is usually negligible and the turbulence production and dissipation are approximately in equilibrium.

The initial assumption of the model is that the air is an incompressible Newtonian fluid with temperature dependent characteristics. Numerical simulation of temperature and calculation of the flow field in numeric domain requires solving the continuity equation (3.1), Reynolds averaged Navier-Stokes equations of motion (3.2) and time-averaged energy equation (3.3), presented in the index tensor notation in the form of:

$$\frac{\partial U_i}{\partial x_i} = 0 \tag{3.1}$$

$$
\begin{aligned}
&\frac{\partial U_i}{\partial t} + U_i \frac{\partial U_j}{\partial x_j} = -\frac{1}{\rho}\frac{\partial P}{\partial x_i} \\
&+ \frac{\partial}{\partial x_j}\left[\nu\left(\frac{\partial U_i}{\partial x_j} + \frac{\partial U_j}{\partial x_i}\right) - \overline{u_i u_j}\right]
\end{aligned} \tag{3.2}
$$

$$
\begin{aligned}
&\rho \frac{DT}{Dt} = \rho \frac{\partial T}{\partial t} + \rho U_j \frac{\partial T}{\partial x_j} \\
&= \frac{\partial}{\partial x_i}\left[\frac{\mu}{\Pr}\frac{\partial T}{\partial x_i} - \rho \overline{\theta u_i}\right]
\end{aligned} \tag{3.3}
$$

Attempts of the numerical calculation of the flow and temperature field of the fluid flow, formed in the case of the jet impinging on a flat heated plate, carried out using standard two-equation turbulence models and standard Reynolds-stress models, showed disagreements with the experimentally determined physical situation. The highest degree of disagreement was observed in the stagnation area of the jets, especially in the calculation of local values of Nusselt numbers.

In the case of two-equation models of turbulence, the reason for these disagreements is usually their known property, to provide relatively wrong predictions for extremely non-isotropic flows. This property is a consequence of their design based on differential transport equations for scalar quantities (k and ε, or k and ω), and the fact that practically all two-equation turbulent models are developed for shear turbulent flows.

Based on the Boussinesq's turbulent viscosity hypothesis, Reynold's stress is a function of the local gradient of velocity and turbulent viscosity ν_t. The coefficient of the turbulent viscosity takes into account viscous interactions of the fluid and is not a physical property of the fluid. By analogy with the constituent relation between the laminar stresses and the deformation rate, the dependence between the turbulent stress and the velocity gradient of averaged fluid flow can be obtained in the form:

$$-\rho\overline{u_i u_j} = \tau_{ij} = \mu_t\left(\frac{\partial U_i}{\partial x_j} + \frac{\partial U_j}{\partial x_i}\right) = \mu_t S_{ij},$$

which is known in the literature as the linear concept of turbulent viscosity. The introduction of the coefficient μ_t (or its kinematic variant ν_t) enables the closure of the system of equations of turbulent motion and the method of its calculation defines the type of model for turbulent flow modelling (μ_t is not a model itself).

In the case of shear turbulent flows, this coincidence and proportionality are more or less present, but in the stagnation zone of the flow generated by impingement of the jet to the surface, the presumption of such dependence is no longer adequate. In this zone, instead of the appearance of the shear, the processes of the fluid particles compression are the dominant ones. This means that those parts of the averaged velocity tensor

responsible for the normal, rather than shear deformations, dominantly change.

If the turbulent stresses for this case of physical fluid flow are modeled in accordance with Boussinesq's hypothesis, this results in a wrong prediction of the turbulence kinetic energy and the linear increase of the corresponding normal turbulent stresses. This erroneous prediction process, for k-ε and k-ω models, is reflected through an enlarged term of the modeled turbulent viscosity, since the increase in the kinetic energy of turbulence causes the turbulent viscosity to increase in proportion to the square of its value.

Energy equation (3.3) has a term $\dfrac{\mu_t}{\mathrm{Pr}}\dfrac{\partial T}{\partial x_i}$, which is not capable to distinguish difference between the effects of certain Reynolds stresses, consequently leads to excessive increase in the enthalpy flow that increase local value Nusselt numbers in the stagnation area.

By moving away from the stagnation point and transformation into the wall jet, the results of numerical calculations are increasingly approaching experimentally measured values. These approximations are not surprising, as with the transition from "non-shear" to a shear turbulent flow, the Boussinesq's hypothesis accurately predicts the relationships between the Reynolds stress tensors and the averaged fluid particle deformation rate tensor. Correctly establishing these relationships leads to an increased accuracy of numerical/mathematical predictions.

In this paper will be shown mathematical models that use turbulent scalar quantities k and ε to calculate v_t, which are obtained by solving the following set of modeled transport equations:

$$U_i \frac{\partial k}{\partial x_i} = \frac{\partial}{\partial x_i}\left[\left(\mu + \frac{\mu_t}{\sigma_k}\right)\frac{\partial k}{\partial x_i}\right]$$
$$+ \mu_t \left(\frac{\partial U_i}{\partial x_j} + \frac{\partial U_j}{\partial x_i}\right)\frac{\partial U_i}{\partial x_j} - \rho\tilde{\varepsilon} \qquad (3.4)$$

$$\rho U_i \frac{\partial \varepsilon}{\partial x_i} = \frac{\partial}{\partial x_i}\left[\left(\mu + \frac{\mu_t}{\sigma_\varepsilon}\right)\frac{\partial \varepsilon}{\partial x_i}\right]$$
$$+ f_1 C_1 \mu_t \frac{\varepsilon}{k}\left(\frac{\partial U_i}{\partial x_j} + \frac{\partial U_j}{\partial x_i}\right)\frac{\partial U_i}{\partial x_j} - \rho f_2 C_2 \frac{\varepsilon^2}{k} \qquad (3.5)$$
$$+ E$$

$$\mu_t = \rho f_\mu C_\mu \frac{k^2}{\varepsilon} \qquad (3.6)$$

$$\tilde{\varepsilon} = \varepsilon + D \qquad (3.7)$$

$$\mathrm{Re}_T = \frac{\rho k^2}{\mu\varepsilon}; \mathrm{Re}_{x_2} = \frac{\rho\sqrt{k}x_j}{\mu};$$
$$\mathrm{Re}_\varepsilon = \frac{\rho(\mu\varepsilon/\rho)^{1/4}x_j}{\mu} \qquad (3.8)$$

where C_μ, C_l, C_2, σ_k and σ_ε are the same empirical constants for turbulent models as those used in k-ε models for large Reynolds numbers. The "dumping functions" f_μ, f_l and f_2, and in some models, the used terms D and E are used to improve the accuracy of the flow model near the wall. The detailed physical meaning of these "dumping functions", as well as terms D and E, with the criteria for determining the correctness of these functions for the flow near the wall are given in the reference Patel et al., 1985 [13].

The modification of the k-ε model for small Reynolds turbulent numbers (so called Low-Reynolds-Number Models) allows their use in the vicinity of the wall. The modification involves inserting a "dumping function" into the original term of the transport equation for ε, and in the expression for turbulent viscosity μ_t.

The "damping functions" allow these equations to be used in a turbulent boundary layer, including a viscous sublayer, but on the other hand they apply only to this case of flow and cannot be applied in other fluid flows.

A modified transport equation for ε (3.5) for using the dumping functions f_μ, f_l and f_2 takes the form:

$$\rho U_i \frac{\partial \varepsilon}{\partial x_i} = \frac{\partial}{\partial x_i}\left[\left(\mu + \frac{\mu_t}{\sigma_\varepsilon}\right)\frac{\partial \varepsilon}{\partial x_i}\right]$$
$$+ \frac{\varepsilon}{k}(f_1 C_{1\varepsilon}\mu_t S^2 - \rho f_2 C_{2\varepsilon}\varepsilon) \qquad (3.9)$$

Low-Reynolds number modification of the basic k-ε model that will be presented in the paper are Abid, 1993, [14], Lam and Bremhorst, 1981, [15], Launder and Sharma, 1974, [16] Abe, Kondoh and Nagano, 1994, [17], and Chang, Hsieh and Chen 1995, [18].

4. RESULTS OF NUMERICAL SIMULATIONS

The subject of numerical analysis in this research was to examine the performance of several different, so called, low-Reynolds number modification of the basic k-ε model (Abid, 1993, Lam and Bremhorst, 1981, Launder and Sharma, 1974, Abe, Kondoh and Nagano, 1994, and Chang, Hsieh and Chen 1995) using commercial CFD code Fluent-Ansys, applied to the problem of jet impinging on a flat surface positioned perpendicular to its propagation.

Application of the low Reynolds number k-ε model modification for this phenomenon requires a very high density of the network with the wall itself, y^+ on a cell at the wall must be at least 1. Preferred optimum is 10 cells in the viscous sub-layer. The calculation was made in double precision coupled solver, and the convergence was achieved when normalized residuals of the dependent variable in the last 10 iterations are less than 10^{-7}.

The geometric model used in the simulations is two-dimensional, and only half of the domain was analyzed due to the axisymmetric nature of the problem. The nozzle diameter is 18 *mm* and the axial distance between the nozzle exit and the impingement surface was varied to obtain *L/D* ratios of 2, 4, 6 and 8, thereby altering the control volume accordingly. The radial distance from the nozzle's axis of symmetry to the outer boundary of the domain is 10*D*. The computational mesh is structured and refined in key regions, particularly near the nozzle exit, in the stagnation region, and along the wall-jet zone. The mesh elements are quadrilateral. Boundary conditions were defined such that air exits the nozzle at a temperature of 300 *K*, with a velocity corresponding to Reynolds numbers of 10000 and 20000, discharging into a quiescent ambient air environment with the same temperature. The impingement surface is modeled as an isothermal wall providing a constant heat flux of 1500 *W/m²* to the fluid. The influence of body forces is considered negligible, and the flow is assumed to be incompressible. To enhance the accuracy of the numerical solution, a second-order discretization scheme was employed.

To characteristics of the jet depending on the excitation Strouhal number suitable for the industrial application here will be presented only fragment of the numerical results. Results of unsteady two-dimensional CFD numerical simulation of pressure fields in the free jet modified by acoustic oscillations, give us the opportunity to analyse the influence of the excitation Strouhal number on the type and character of vortex structures on the periphery of the jet that occur as a result of these modifications. Time step in the numerical calculation is carefully selected to strictly reproduce the entire sinusoidal change of jet velocity, depending on the Strouhal number of the excitation [19, 20].

On Figure 7. are shown pressure fields in a free jet (in the selected time) in the case of the Reynolds number Re_D=10000 modified by acoustic oscillations with Strouhal number St_D=0.3, 0.6 and 2.0 and the oscillation amplitude of 20%. Only one half of the jet issuing from the nozzle (bottom left side of Figures) is presented due to the axisymmetry of the problem.

From pathlines of the pressure shown above, representing different excitation conditions with Strouhal number St_D=0.3, 0.6 and 2.0, can be clearly seen shape and size of vortices formed due to excitation modification. Numerical simulation confirmed that conclusions derived from experimental analysis given in previous chapters are correct.
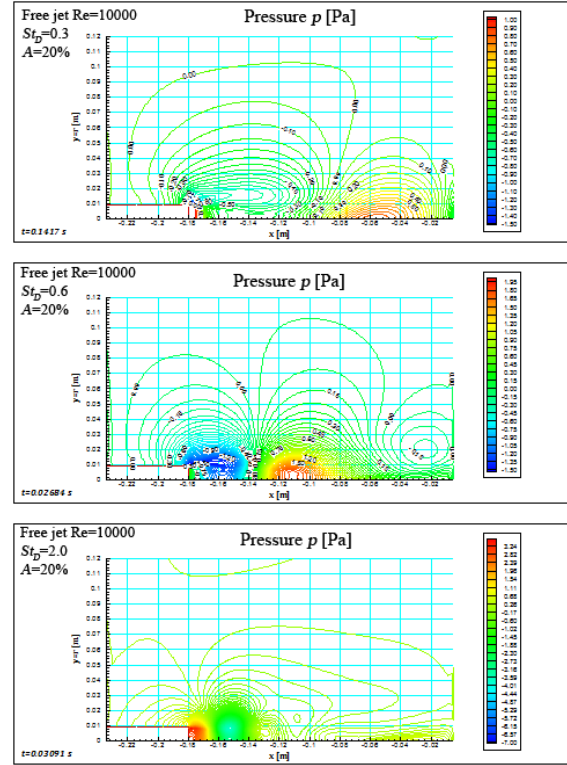

Figure 7. Pressure field in the sound modified turbulent axisymmetric jet; *Re*=10000; *St_D*=0.3-2.0

Numerical simulation of the excitation case with Strouhal number St_D=2.0 showed that train of vortices small in size formed at the nozzle lip, are very fast disintegrated in the area close to the nozzle making uniformity in the field on a larger axial distance. This analysis also confirms that this excitation range around Strouhal number St_D=2.0 can be very interesting for applications.

It is noted that the agreement with the experimental results is very good at all distances from the jet axis, for which it is certainly because of the inlet velocity setting based on the experimentally determined values. As the analysis of the profiles from Figure 8. can be concluded, the software does not provide calculations in cells that are close to the wall of the impact plate, but it uses a wall function that contains a dumping function that is characterized by each of the tested modifications of the *k-ε* model.

The calculation is not conducted in the whole area in the vicinity of the wall (from the image shows that the first cell of which enter into the calculation at a distance x_2/D=0.025) so that the observed differences in the cells just above the wall zone can be ascribed to the very method of calculation. When further away from the impact plate, the velocity profile follows the profile of the measured values in a satisfactory accuracy.

It may be noted that all five tested modifications of the standard *k-ε* model shows some differences in averaged velocity profiles at four radial cross-

sections shifted from the axis of the jet shown in Figure 8. This was to be expected, since all five modifications k-ε models have the same constants of the k-ε model, and differ only in the applied coefficients characterized by the "damping" functions, so that the differences can be expected in the profiles of the production of turbulence kinetic energy and the coefficient of heat transfer.
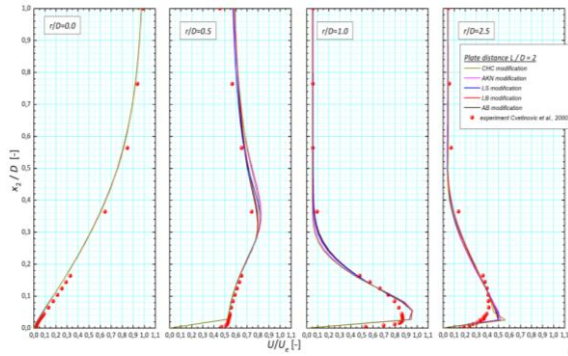

Figure 8. Averaged velocity profiles for Re_D = 20000, L/D = 2; Comparison of own experimental results with numerical simulation results for five modifications of the k-ε model for low Reynolds turbulent numbers

Changes in the value of local Nusselt number (for comparison with other authors in the form of $Nu/Re^{0.7}$) for several distances from the nozzle are given in the following figures, Figure 9-12.
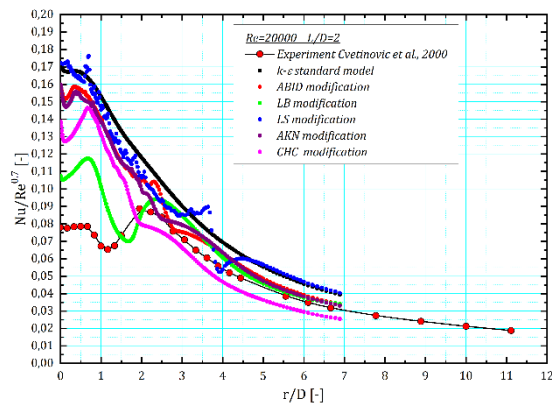

Figure 9. Local Nusselt number profiles for Re_D = 20000, L/D = 2; Comparison of own experimental results with numerical simulation results for five modifications of the k-ε model for low Reynolds turbulent numbers

Calculated heat transfer coefficients in the case of the smallest distance of the impinging surface from the nozzle outlet L/D=2 are given in Figure 9. In general, all 5 modifications of the standard k-ε turbulence model for low Reynolds turbulent numbers improve the prediction of local heat transfer coefficients in the impact zone jet against the base model. However, the prediction also exceeds the values of the Nusselt numbers determined experimentally in the r/D<2 zone. It can be noticed that some of the proposed modifications and numerically unstable, there was a slight divergence of the solution. There is a particularly notable disagreement with experimentally determined values at higher radial distances from the jet stream which is unacceptable and can be explained by poor selection of damping functions and/or the lack of a justified criterion in the calculation for the application of "damping functions" whose role is to damp production of the kinetic turbulence energy in this zone.

By moving the impinging surface to greater distances from the nozzle outlet, the results of the calculation approach the measured values, as can be seen in Figure 10., which represents the calculated values of the local heat transfer coefficients in the case of distance L/D = 4 from the impinging plate from the output from nozzle.
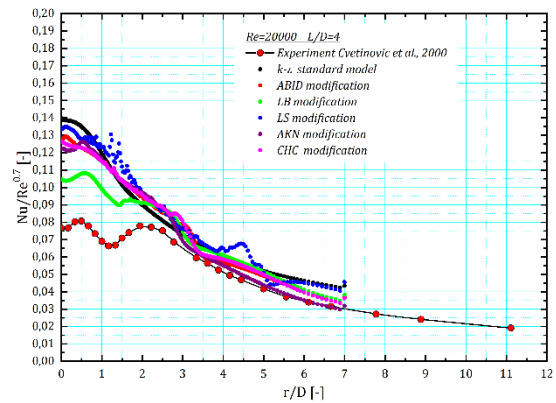

Figure 10. Local Nusselt number profiles for Re_D = 20000, L/D = 4; Comparison of own experimental results with numerical simulation results for five modifications of the k-ε model for low Reynolds turbulent numbers

The presented results of calculations of the distance L/D = 4 still above the measured but still can claim to better anticipate local Nusselt numbers of basic k-ε model in the stagnation zone of the jet. Calculations instability is retained in some modifications of the standard turbulence model for low Reynolds turbulent numbers, which is also reflected in the jumps at some of the radial distributions shown in Figure 10. Also, the observed distributions indicate a deviation from the measured values at higher radial distances from the jet axis.

For larger distances of the impinging surface from the outlet of the nozzle of L/D = 6 and 8, shown in Figures 11. and 12., it is evident much better agreement with the measured values and, also, evident improvement over the standard k-ε turbulence model.
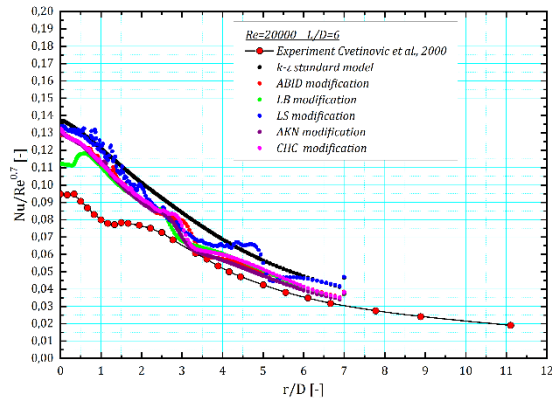
Figure 11. Local Nusselt number profiles for Re_D = 20000, L/D = 6; Comparison of own experimental results with numerical simulation results for five modifications of the k-ε model for low Reynolds turbulent numbers
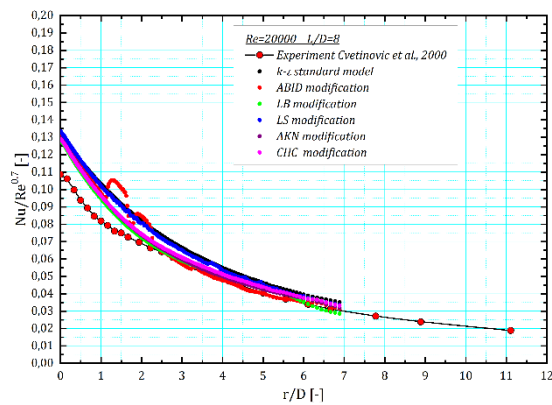

Figure 12. Local Nusselt number profiles for Re_D = 20000, L/D = 8; Comparison of own experimental results with numerical simulation results for five modifications of the k-ε model for low Reynolds turbulent numbers

The objective of the numerical investigation of the heat transfer from a turbulent axisymmetric jet to a flat surface that was set up normally on the jet centerline was to examine the performance and possibilities in predicting local Nusselt numbers of the simplest two-equation turbulence models, and by several authors of the proposed modifications of the standard two-equation k-ε turbulence model for low Reynolds turbulent numbers.

Although the prediction of the local heat transfer coefficients over predicts the experimental data, better predictive results have been achieved than some that are listed in the literature. The reason for this is in the carefully given input parameters in the calculations corresponding to the experimental results with which the comparison was made.

5. CONCLUSIONS

Stagnation heat transfer can be augmented by increasing not only the time averaged approach velocity and turbulence intensity but also the characteristic frequency of the jet to hit the impinging surface with large-scale vortical structure, which is the main characteristic of the late-transitional region of the jet. Large-scale eddies on the heat transfer target surface intermittently impinge onto the boundary layer around the stagnation point. Such areas can be considered to have adverse gradients of the instantaneous surface pressure very often because the gradients of the time averaged surface pressure are almost zero there. If a target plate is situated in the transitional region of a turbulent free jet, therefore, unsteady separation-like reverse flow could occur at and near the stagnation point owing to the intermittent impingement of large-scale vortical structures on the target plate.

In this paper was demonstrated the ability to control eddy structure in the axisymmetric turbulent jet by sound modulations of jet velocity at the exit of the nozzle as an attractive possibility to be used in the technological processes. In fact, sometimes it is necessary to intensify the mixing of primary fluid flow and the surrounding fluid (in the chemical reactor), by sound modulation which intensifies eddy structures in a jet shear layer, while, for example, to achieve uniformity of the heat transfer coefficient on a major surface of the impinging surface it is necessary to apply modulation with totally different frequency.

The objective of the numerical investigation of the heat transfer from a turbulent axisymmetric jet to a flat surface that was set up normally on the jet centerline was to examine the performance and possibilities in predicting local Nusselt numbers of the simplest two-equation turbulence models, and by several authors of the proposed modifications of the standard two-equation k-ε turbulence model for low Reynolds turbulent numbers.

Prediction of the local heat transfer coefficients is better than some that are listed in the literature. The reason for this is in the carefully given input parameters in the calculations corresponding to the experimental results with which the comparison was made. This study can serve as a base for development and optimization of the technological processes that involve air jet.

REFERENCES

[1] Jambunathan, K., Lai, E., Moss, M. A., Button, B. L., 1992: A review of heat transfer data for single circular jet impingement, *International Journal of Heat and Fluid Flow*, vol. 13, no. 2, pp. 106-115

[2] Zuckerman, N. and Lior, N., 2006: Jet impingement Heat Transfer: Physics, Correlations and Mathematical Modelling, *Advances in Heat Transfer*, Volume 39, ISSN: 0065-2717, DOI: 10.1016-S0065-2717(06)39006-5, pp. 565-631

[3] Behnia, M., Parneix, S., Durbin, P. A., 1998: Prediction of heat transfer in an axisymmetric turbulent jet impinging on a flat plate, *International Journal of Heat and Mass Transfer*, vol. 41, no. 12, pp. 1845-1855

[4] Chen, H., Chong, K. L., 2025: Heat transfer mechanisms in impinging jets: The role of vortex dynamics, *International Journal of Heat and Mass Transfer*, vol. 248, Article 127142

[5] Rönnberg, K., Duwig, C., 2021: Heat transfer and associated coherent structures of a single impinging jet from a round nozzle, *International Journal of Heat and Mass Transfer,* vol. 173, Article 121197

[6] Cvetinovic D., Tihon J., Verjazka J., Drahos J., 2004: "Effect of external excitations on the axisymmetrical air jet flow structures - Investigations of the Free Jet", *CHISA 2004*, 22-26. August 2004, Prague, Czech Republic, P5.237, ISBN 80-86059-40-5

[7] Cvetinovic D., Tihon J., Verjazka J., Drahos J., 2004: "Effect of external excitations on the axisymmetrical air jet flow structures - investigations of the jet impinging on a flat surface", *CHISA 2004*, 22-26. August 2004, Prague, Czech Republic, P5.236, ISBN 80-86059-40-5

[8] Hussain A.K.M.F. and Hasan M.A.Z., 1983: The "Whistler-nozzle" Phenomenon, *J. Fluid Mech.*, vol. 134, pp. 431-458

[9] Zaman, K. B. M. Q., Hussain, A. K. M. F., 1980: Vortex pairing in a circular jet under controlled excitation, Part 1. General jet response, *Journal of Fluid Mechanics*, vol. 101, part 3, pp. 449-491

[10] Hussain, A. K. M. F., Zaman, K. B. M. Q., 1980: Vortex pairing in a circular jet under controlled excitation. Part 2. Coherent structure dynamics, *Journal of Fluid Mechanics*, vol. 101, part 3, pp. 493-544

[11] Hussain, A. K. M. F., 1986: Coherent structure and turbulence, *Journal of Fluid Mechanics*, vol. 173, pp. 303-356

[12] Suresh, P. R., Srinivasan, K., Sundararajan, T., Das, Sarit K., 2008: Reynolds number dependence of plane jet development in the transitional regime, *Physics of Fluids*, vol. 20, Article 044105

[13] V. C. Patel, W. Rodi and G. Scheuerer: Turbulence Models for Near-Wall and Low Reynolds Number Flows: A Review August 1985, *AIAA Journal* 23(9):1308-1319, https://doi.org/10.2514/3.9086

[14] Abid, R., 1993: Evaluation of two-equation turbulence models for predicting transitional flows, *International Journal of Engineering Science* 31 (6) (1993) 831–840.

[15] Lam, C.K.G., Bremhost, K., 1981: A modified form of the k–ε model for prediction wall turbulence, *Transactions of the ASME, Journal of Fluids Engineering* 103 (1981) 456–460.

[16] Launder, B.E., Sharma, B.I., 1974: Application of the energy-dissipation model of turbulence to the calculation of flow near a spinning disc, *Letters in Heat and Mass Transfer* 1 (1974) 131–138.

[17] Abe, K., Kondoh, T., Nagano, Y., 1994: A new turbulence model for predicting fluid flow and heat transfer in separating and reattaching flows I: Flow field calculations, *International Journal of Heat and Mass Transfer* 37 (1) (1994) 139–151.

[18] Chang, K.C., Hsieh, W.D., Chen, C. S., 1995: A modified low-Reynolds-number turbulence model applicable to recirculating flow in pipe expansion, *Transactions of the ASME, Journal of Fluids Engineering*, 117, pp. 417–423.

[19] Cvetinović D. B., Stefanović P. Lj., Bakić V. V., Oka S. N., Review of the research on the turbulence in the laboratory for thermal engineering and energy, Thermal Science 2017 Volume 21, Issue suppl. 3, Pages: 875-898, doi: 10.2298/TSCI160221330C

[20] Cvetinović D. B., Ćetenović N. M., Erić A. M., Anđelković J. D., Čantrak Đ. S., Transient modeling of impinging heat transfer from an acoustically modulated turbulent air jet to a normally positioned flat surface, Thermal Science 2025 Volume 29, Issue 1 Part B, Pages: 767-780, doi: 10.2298/TSCI2501767C